International Journal of the Physical Sciences Vol. 6(3), pp. 566-576, 4 February, 2011
Available online at http://www.academicjournals.org/IJPS
DOI: 10.5897/IJPS11.004
ISSN 1992 - 1950 ©2011 Academic Journals

Full Length Research Paper

Comparison between Mahalanobis classification and neural network for oil spill detection using RADARSAT-1 SAR data

Maged Marghany* and Mazlan Hashim

Institute of Geospatial Science and Technology (INSTEG), UniversitiTeknologi Malaysia 81310 UTM, Skudai, JohoreBahru, Malaysia

Accepted 19 January, 2011

Oil spill or leakage into waterways and ocean spreads very rapidly due to the action of wind and currents. The study of the behavior and movement of these oil spills in sea had become imperative in describing a suitable management plan for mitigating the adverse impacts arising from such accidents. But the inherent difficulty of discriminating between oil spills and look-alikes is a main challenge with Synthetic Aperture Radar (SAR) satellite data and this is a drawback, which makes it difficult to develop a fully automated algorithm for detection of oil spill. As such, an automatic algorithm with a reliable confidence estimator of oil spill would be highly desirable. The main objective of this work is to develop comparative automatic detection procedures for oil spill pixels in multimode (Standard beam S2, Wide beam W1 and fine beam F1) RADARSAT-1 SAR satellite data that were acquired in the Malacca Straits using two algorithms namely, post supervised classification, and neural network (NN) for oil spill detection. The results show that NN is the best indicator for oil spill detection as it can discriminate oil spill from its surrounding such as look-alikes, sea surface and land. The receiver operator characteristic (ROC) is used to determine the accuracy of oil spill detection from RADARSAT-1 SAR data. The results show that oil spills, lookalikes,and sea surface roughness are perfectly discriminated with an area difference of 20% for oil spill, 35% look–alikes, 15% land and 30% for the sea roughness. The NN shows higher performance in automatic detection of oil spill in RADARSAT-1 SAR data as compared to Mahalanobis classification with standard deviation of 0.12. It can therefore be concluded that NN algorithm is an appropriate algorithm for oil spill automatic detection and W1 beam mode is appropriate for oil spill and look-alikes discrimination and detection.

Key words: Oil Spill, RADARSAT-1 SAR data, Mahalanobis classification, neural network (NN).

INTRODUCTION

Standard procedures are required for oil spill detection from multi SAR data to ensure the coastal zone clean up. These procedures can be of benefit to international oil companies like Brega Marketing Company in Libya (Middle East) and Petronas (Malaysia). Rapid information on pollutant substances that exist on the sea is necessary for coastal management to avoid damage to marine ecosystem. In addition, the improvement of coastal tourism requires the involvement of many parties such as local inhabitants, policy makers, and the scientific community (Siry, 2007). Policy makers play an important role by issuing regulations and policies that guide the design of sites for tourist and support facilities like hotels and recreational areas. In designing such sites, designers need accurate information which could be supplied by microwave radar data (Marghany and Mazlan, 2010). According to Marghany (2004), policy makers are required to make the decision more comprehensible by involving scientists.

*Corresponding author: E-mail: maged@utm.my, magedupm@hotmail.com.

Oil spill pollution has a substantial role in damaging marine ecosystem. Oil spill that floats on top of water, as well as decreasing the fauna populations, affects the food chain in the marine ecosystem (Dunnet et al., 1982). In fact, oil spill is reducing the amouint of sunlight that penetrates the water, limiting the photosynthesis of marine plants and phytoplankton. Moreover, marine mammals for instance, disclosed to oil spills a reduction of their insulating capacities, and so making them more vulnerable to temperature variations and much less buoyant in the seawater. Dunnet et al. (1982) stated that oil coats the fur of sea otters and seals, reducing its insulation abilities and leading to body temperature fluctuations where the body temperature is much lower than normal (hypothermia). Ingestion of the oil causes dehydration and impaired digestions (Fingas, 2001; Zeynalova et al., 2009).

Oil spill pollution causes political and scientific concerns because they have serious effects on feeble maritime and coastal ecologies. Significant parameters in evaluating seawater quality are the amounts of pollutant discharged and associated effects on the marine environment (Topouzelis, 2008). There are many sources of oil pollution and spillage, which may be as a result of exploitation, extraction, transportation, and/or disposal activities. In the case oil pollution occurrence in marine environment, the first undertaken task is determination of priorities for protection against pollution. According to Fingas (2001), more than 75% of sea pollution is manmade (Marghany and Genderen, 2001; Brekke and Solberg, 2005). Each year, around 48% of oil pollution in the oceans is from fuels, 29% is from crude oil, while tanker accidents contribute only 5% (Zeynalova et al., 2009).

Remote sensing technology is a valuable source of environmental marine pollution detection and surveying that improves oil spill detection by various approaches. The different tools to detect and observe oil spills are vessels, airplanes, and satellites (Brekke and Solberg, 2005). Vessels can detect oil spills at sea, covering restricted areas, say for example, (2500 × 2500 m), when they are equipped with navigation radars. On the other hand, airplanes and satellites are the main tools that are used to record sea-based oil pollution (Topouzelis, 2008). Recently, scientists and researchers have reported the fluorescent Lidar as a promising technique for oil spill detection, because of its high capability to perform actively and can positively distinguish oil from biological substances and surrounding sea environment. According to Holt (2004), most organic multi-party compounds have individuality of the fluorescence production spectrum. Hence, fluorescence emission is a strong indication of the presence of oil. On the other hand, most huge systems installed on large airplanes are seldom use as tool for oil pollution cleanup (Hengsterman and Reuter, 1990; Balick et al., 1997).

Further Brekke and Solberg (2005) reported that the most applicable space-borne sensor for oil spill detection is synthetic-aperture radar (SAR). SAR sensors perform in all-weather conditions and provide all-day detection coverage. Again, SAR satellite data can penetrate the cloud covers because of its independence on sun radiation (Trivero et al., 2001), and also can operate at wind speeds of up to 12 to14 m/s depending on oil type and age. Sensors operating in wide strip modes with a resolution of 50 to 150 m are found to be satisfactory and efficient in covering large ocean areas (Topouzelis et al., 2008).

Most scientists have shown great interest in the huge maritime environmental damage due to oil slicks, which have increase pollution effects greatly. Space-borne RADARSAT-1 SAR images are used to monitor and control oil slicks, however, the main challenges lies in the difficulties inherent in discriminating between oil spills and look–alikes. According to Marghany and Hashim (2005) both appears as a dark spot in SAR data. Also according to Alpers and Hühnerfuss (1988); Trivero et al. (1998), the existence of an oil layer on the sea surface damps the small waves which increase the thickness of the top film and this significantly decreases the measured backscattering energy resulting in darker areas in SAR imagery. The European remote sensing satellite (ERS) task is an example of SAR.

However, Frate et al. (2000), argued that careful analysis is required since the dark areas might also be generated by local low winds or by normal sea slicks. Researchers such as Solberg et al. (1999); Brekke and Solberg (2005); Topouzelis (2008), agreed that well tuned classification algorithms can be employed to avoid false alarms. Oil spills show a larger discontinuity effect on the environment, mainly because of its thickness. A possible procedure could be formulated based on the selection of an area in an image containing dark pixels; computation of physical and geometrical features characterizing an object; classification of the object into oil spill or look-alike, based on the dark spot texture (Brekke and Solberg, 2005; Topouzelis et al., 2008).

The main objective of this work is to develop comparative detection procedure of oil spills using multimode RADARSAT-1 SAR satellite data. This objective is divided into the following sub-objectives:

(i). To examine various algorithms such as Mahalanobis classifier; and artificial intelligence techniques for oil spill automatic detection in multimode RADRASAT-1 SAR data.
(ii) To determine an appropriate algorithm for oil spill automatic detection in multimode RADRASAT-1 SAR data that is based on algorithm's accuracy (Solberg et al., 1999).

RESEARCH METHODS

Study area

The study is carried out along the Malacca Straits coastal waters. The Strait of Malacca is located between the east coast of Sumatra

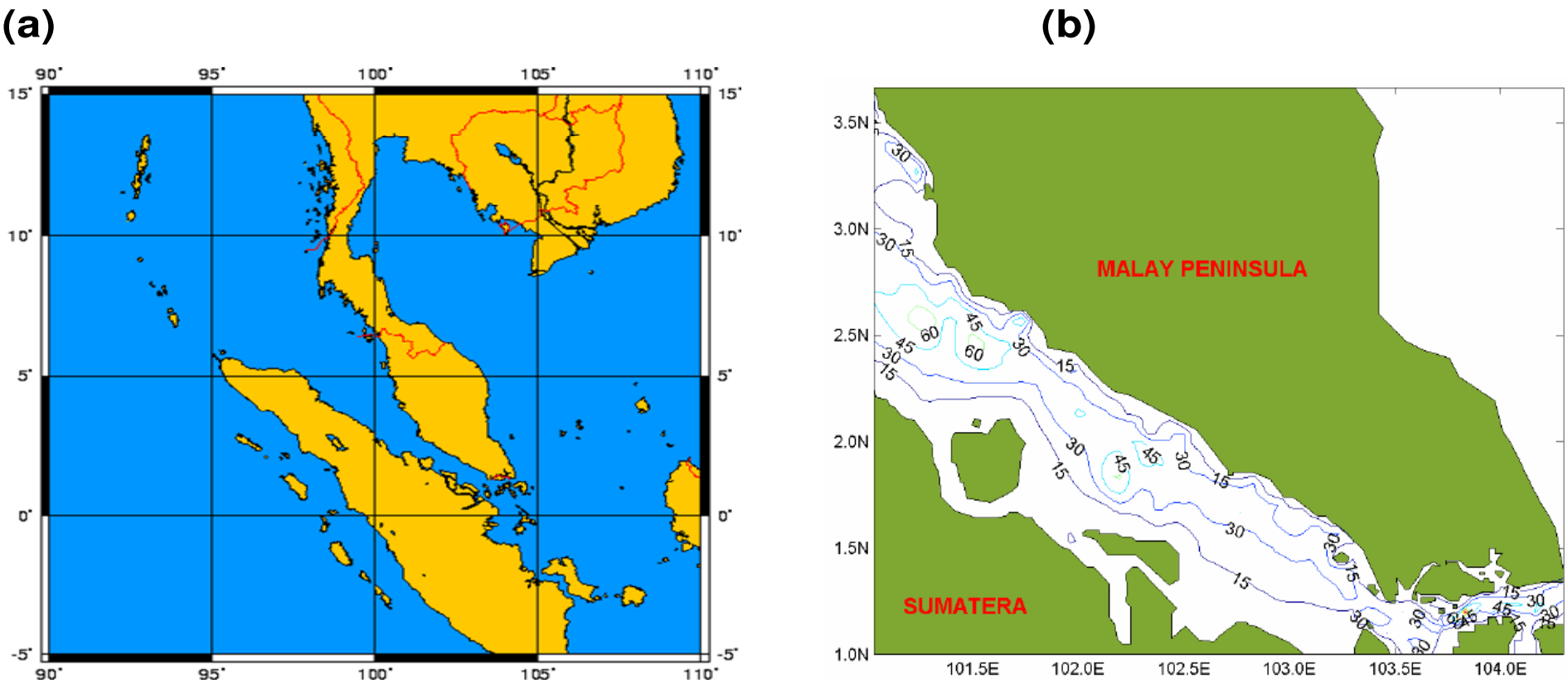

Figure 1. (a) Map of Malacca Straits (b) Coastal Bathymetry.

Island in Indonesia and the west coast of Peninsular Malaysia, and is linked with the Strait of Singapore at its south-east end (Figure 1a). The Strait of Malacca is bordered on the north-west by a line from Ujung Baka (5°40 ′N, 95°26′ E),the north-west extremity of Sumatra, to Laem Phra Chao(7°45 ′N,98°18 ′E),the south extremity of Ko Phukit Island, Thailand and on the south-east by a line from Tahan (Mount) Datok (1°200′ E,104°20′ N) and Tanjung Pergam (1°100′ E, 104°20′ N) (Hamzah, 1988; Marghany 2001).

The Malacca Straits is dominated by tropical climate. The different monsoon periods are influenced by the weather of the Malacca Straits. The heavy rain season is main feature on northeast monsoon period which brings rain from December to February, whereas, the dry season which is represented by the southwest monsoon period and starts from May to August (Marghany, 2001; Marghany and Hashim, 2010; Marghany, 2010; Marghany et al., 2010). According to Marghany (2010), the weather is unpredictable during the inter-monsoon period. Figure 1b shows a shallow water bathymetry which is dominant feature in the Malacca Straits. The water bathymetry ranges from 5 to 60 m and moves parallel to coastline of Malaysia.

Data acquisition

The SAR data acquired in this study are from the RADARSAT-1 SAR that involves Standard beam mode (S2); W1beam mode (F1) image (Table 1). SAR data are C-band and have a lower signal-to noise ratio due to their HH polarization with wavelength of 5.6 cm and a frequency of 5.3 GHz. Further, RADARSAT-SAR data have 3.1 looks and cover an incidence angle of 23.7 and 31.0° (Marghany et al., 2009a, b). In addition, RADARSAT-SAR data cover a swath width of 100 km. According to Marghany (2001), and Marghany et al. (2009a, b) oil spill occurred on 20

Table 1. RADARSAT-1 SAR satellite data acquisitions.

Mode type	Resolution (m)		Incident Angle(°)	Looks	Swath width (km)	Date
	Range	Azimuth				
W1	182.437	150.000	20° - 5°	1 x 4	100 km	1997/10/26
S2	111.662	110.037	20° - 41°	1 x 4	100 km	1999/12/17
F1	113.675	137.675	37° - 49°	1 x 1	50 km	2003/12/11

December 1999, along the coastal water of Malacca Straits.

Classification procedures

Mahalanobis classification procedures were adopted. This algorithm is based on a correlation between variables by which different patterns can be identified and analyzed. It is a useful way of determining similarity of an unknown sample set to a known one. It differs from Euclidean distance in that it takes into account the correlation of the data set and is scale – invariant, that is, not dependent on the scale of measurement (Brekke and Solberg, 2005). Formally, the Mahalanobis distant of a multivariate vector is given as:

$$D_{M_{(v)}} = \sqrt{(v-\mu)^T S^{-1}(v-\mu)} \quad (1)$$

where $V=(v_1, v_2, v_3.....,v_n)^t$ from group of values with mean $\mu=(\mu_1, \mu_2, \mu_3.....,\mu_n)^t$, and S, is covariance matrix.

In order to apply Mahalanobis classification procedures to different remote sensing data, let v be the feature vector for the unknown input, and let M_1, M_2 be the two classes: oil spill, and look-alike. Then the error in matching v against M j is given by [v- M_j], the Euclidean distance. A minimum-error classifier computes [v- m_j] for *j*= 1 to 2 and chooses the class for which this error is minimum (Figure 2).

If the covariance matrix is the identity matrix, the Mahalanobis distance reduces to the Euclidean distance. If the covariance matrix is diagonal, then the resulting distance measure is called the normalized Euclidean distance:

$$d = (\vec{v})\sqrt{\sum_{i=1}^{n} \frac{v_i^2 - v_j^2}{\delta_i^2}} \quad (2)$$

where δ_i is the standard deviation of the v_i over the sample set.

The input parameters from SAR data can impact the Mahalanobis classifier running when the variability inner classes is smaller than whole classifier group variabilities. In this context, if the classes M are badly scaled and the decision boundaries between classes are curved, the classifier accurcy is reduced. Some of the limitations of simple minimum-Euclidean distance classifiers can be overcome by using the Mahalanobis distance d_t^2 that in covariance matrix C form is;

$$d_t^2 = (v-M_j)c^{-1}(v-M_j) \quad (3)$$

AI techniques for oil spill automatic detection

The general framework of the AI techniques used in this work is elaborated in Figure 3.

In Figure 3, v_1, v_2, v_3 and v_n are assumed as input pixel values from SAR data of different dark patch pixels. Figure 4 shows that the input vectors for the artificial neural network (ANN) are backscatter variation values from dark spot patches and their surrounding environment pixels in SAR data, while the output layer is oil spill or look-alikes. The output is the automatic level detection in the range between 0 and 1. In this context, oil spill pixels are represented by 1 while look-alikes or wind low zone pixels are represented by 0. The neural network (NN)-based pattern-recognition approach for Static Security Assessment (SSA) depends on the assumption that there are some characteristics of pre-contingency system states that give rise to oil spill occurrences in RADARSAT-1 SAR data which is represent post-contingency system**.** The task of the NN is to capture these common underlying characteristics for a set of known operating states and to interpolate this knowledge to classify a previously unencumbered state. The first step in such an application is to obtain a set of training data which represents the different backscatter value variations in RADARSAT-1 SAR data (Topouzelis et al., 2008).

Following, Hect-Nielsen (1989) and Topouzelis et al. (2009), the ANN's and the pattern recognition (PR) technique, feed forward network with back-propagation algorithm are used in this study for both static and dynamic security assessment. For this application, a multi-layer feed forward network with error back-propagation has been employed (Aggoune et al., 1989). The major steps in the training algorithm are: Feed forward calculations, propagating error from output layer to input layer and weight updating in hidden and output layers (Frate et al., 2000). Forward pass phase calculations are shown by the following equations between input (i) and hidden (j) (Michael, 2005 and Topouzelis et al., 2009).

$$\theta_j = \frac{1}{1+e^{(\sum_j w_{ij}\theta_i+\theta_j)}} \quad (4)$$

$$\theta_k = \frac{1}{1+e^{(\sum_k w_{jk}\theta_j+\theta_k)}} \quad (5)$$

where θ_j is the output of node *j*, θ_i is the output of node *i*, θ_k is the output of node w_{jk} is the weight connected between node *i*and *j*, and θ_j is the bias of node *j*, θ_k is the bias of node k.

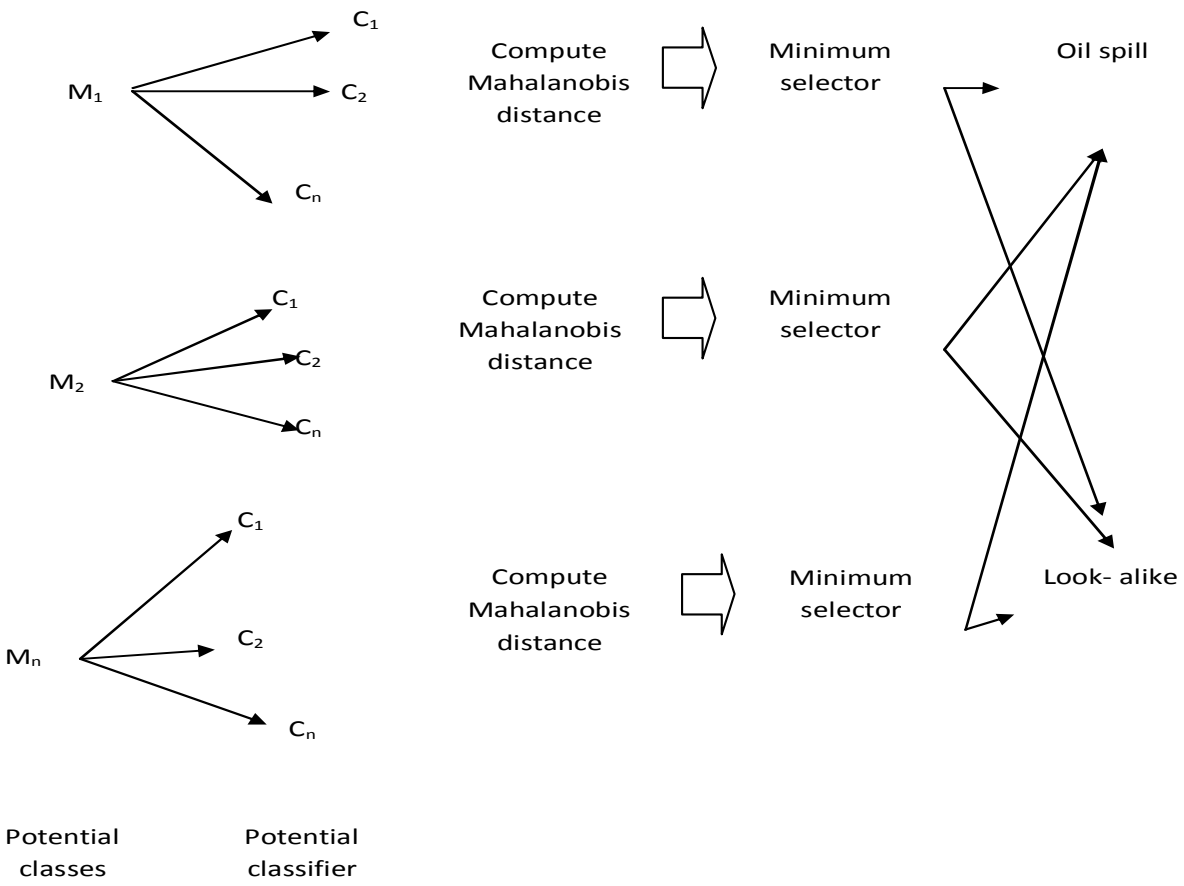

Figure 2. Logical operation of detection oil spill using Mahalanobis classifier.

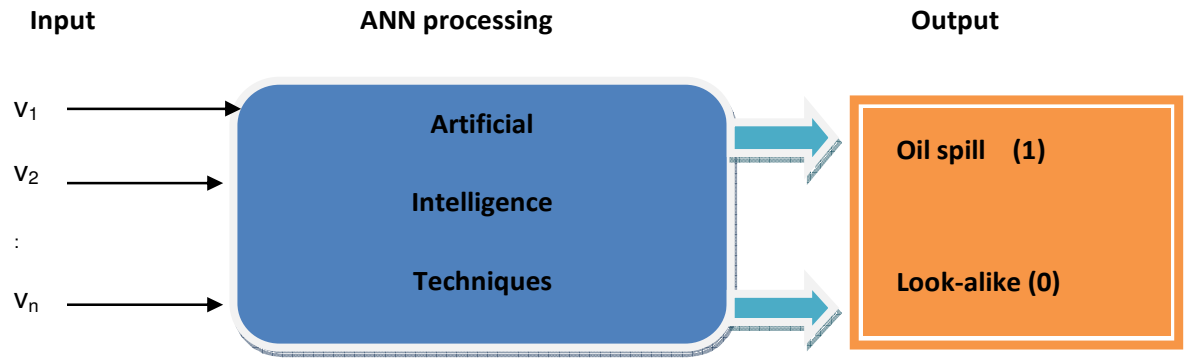

Figure 3. General framework of the AI techniques.

In backward pass phase, error propagated backward through the network from output layer to input layer as represented in Equation 6 (Michael, 2005). Following Topouzelis et al. (2009), The weights are modified to minimize mean square error (MSE).

$$MSE = \frac{1}{n}\sum_{i=1}^{n}\sum_{j=a}^{m}(d_{ij} - y_{ij})^2 \quad (6)$$

where d_{ij} is the j^{th} desired output for the i^{th} training pattern, and y_{ij} is the corresponding actual output.

More details of the mathematical procedure are available in Michael (2005). Finally, the receiver-operator-characteristics (ROC) curve and error standard deviation are used to determine the accuracy level of each algorithm been used in this study. In

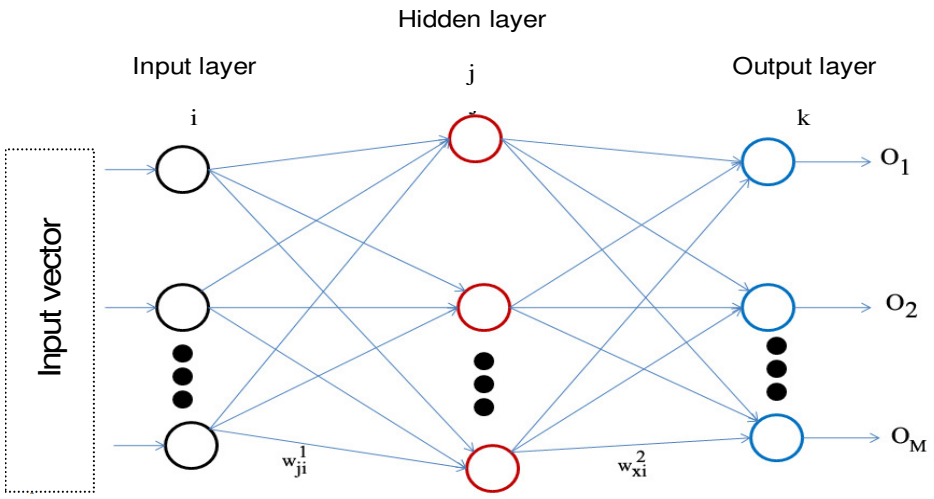

Figure 4. Structure of multilayered feed forwards neural network.

addition, ROC and error standard deviation was used to determine the accuracy of feature detections in RADARSAT-1 SAR data. These methods have been described (Marghany et al., 2009b).

RESULTS AND DISCUSSION

Figure 5 shows the output results of Mahalanobis classification with different RADARSAT-1 SAR mode data. Initial results indicate obvious discriminations between oil spill, look-alikes and low wind zone. Figures (5a) and (5c) show that the oil spill has a large contrast to the gray-values of surrounding pixels. In fact, the surrounding areas are homogenous, with a constant gray-level.

Mahalanobis classification can identify oil spill pixels from the surrounding environment (Migliaccio et al., 2007). This classification uses the training data by estimating means and variances of the classes, which are used to estimate probabilities and also consider the variability of brightness values in each class. It is the most powerful classification methods when accurate training data is provided and one of the major widely used algorithms (Fiscella et al., 2000). Figures (5a) and (5c) shows that the slick has a large contrast to the gray-values surroundings. The surrounding areas are homogenous, with a constant gray-level. Further, Mahalanobis classifier provides excellent identification of oil spill pixels as with the high accuracy level of 87.8 and 92.7%, using Mahalanobis regularized Mahalanobis classifier respectively (Figure 6).

In addition, Figures 5a and 5c shows the ability of Mahalanobis classification in determing the level of oil spill spreadings. In this context, this classification uses the training data by estimating means and variances of the classes, which are used to estimate the probabilities and also consider the variability of brightness values in each class (Fiscella et al., 2000). These results are confirm the previous study of Brekke and Solberg (2005).

It is clear that neural network algorithm is able to isolate oil spill dark pixels from the surrounding environment. In other words, look-alikes, low wind zone, sea surface roughness, and land are marked by white colour while oil spill pixels are marked all black. Figure (7b) does not show any class presence or existence of oil spill event. Further, Figure 7a and 7c shows the results of the Artificial Neural Net work, where 99% of the oil spills in the test set were correctly classified. Three scenes by the leave-one-out method presented an exact classification of 99% for oil spills (an approach based on multilayer perceptron (MLP) neural network with two hidden layers). The net is trained using the back-propagation algorithm to minimize the error function. 99% of oil spills are automatically detected using the leave-one-out method. This study agrees with study of Topouzelis et al. (2009).

The receiver –operator characteristics (ROC) curve in Figure 8 indicates significant difference in the discriminated between oil spill, look-alikes and sea surface roughness pixels. In terms of ROC area, oil spill has an area difference of 20 and 35% for look –alike and 30% for sea roughness and a ρ value below 0.005 which confirms the study of Marghany and Mazlan (2005). This suggests that Mahalanobis classifier and neural net works are good methods to discriminate regions of oil slicks from surrounding water features.

Figure 9, however, shows the standard deviation of the estimated error for neural net work of value 0.12 is lower than the Mahalanobis. This suggests that ANN performed accurately as automatic detection tool for oil spill in RADARSAT data. The good performance of the neural algorithm encouraged a second phase where an optimization of the net from the point of view of the

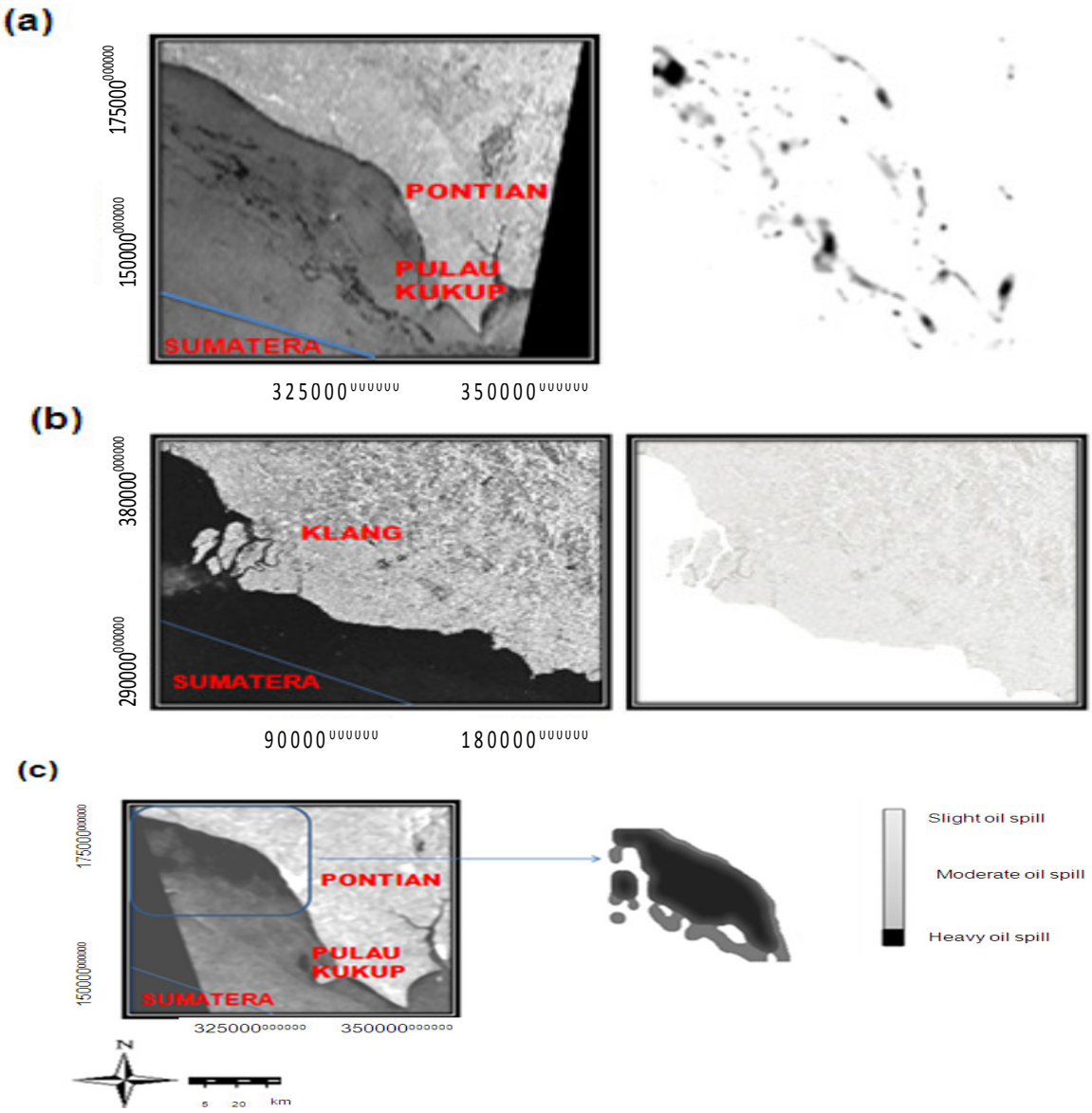

Figure 5. Mahalanobis classifier (a) wide mode (W1), (b) standard mode (S2) and (c) fine mode (F1) data.

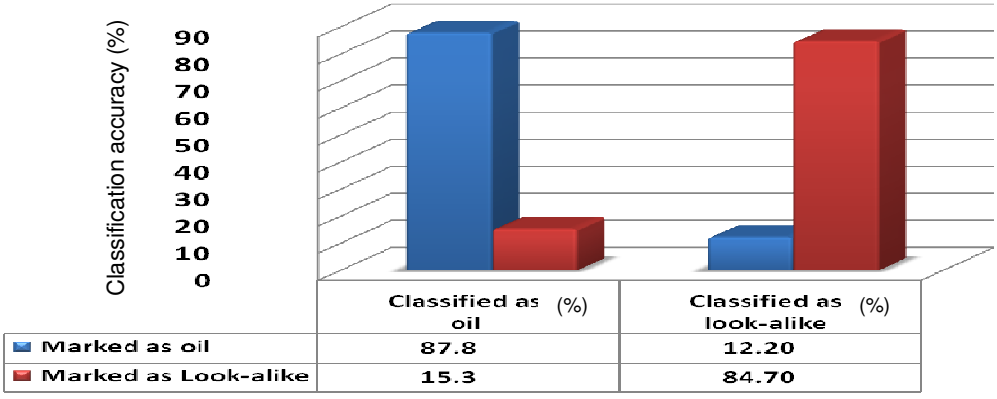

Figure 6. Accuracy of Mahalanobis classification results.

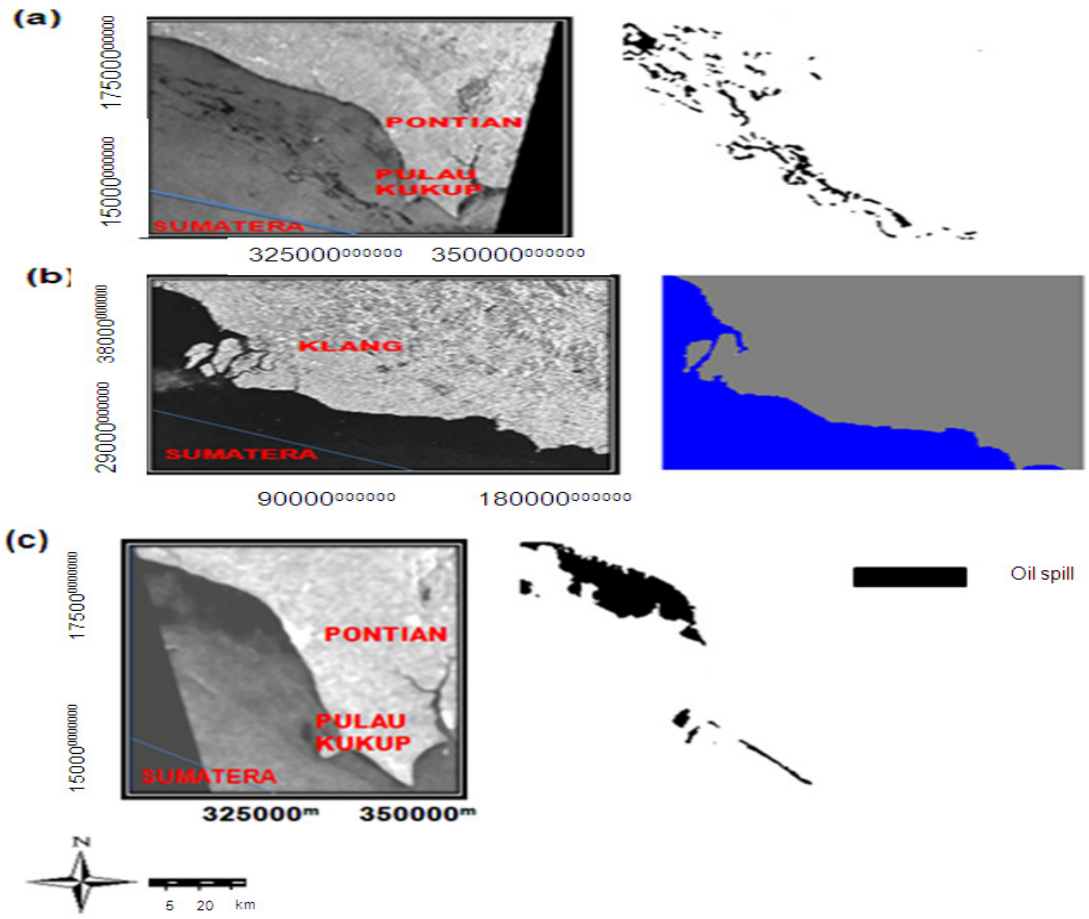

Figure 7. Neural network for automatic detection of oil spill from (a) W1, (b) S2, and (c) F1 mode data.

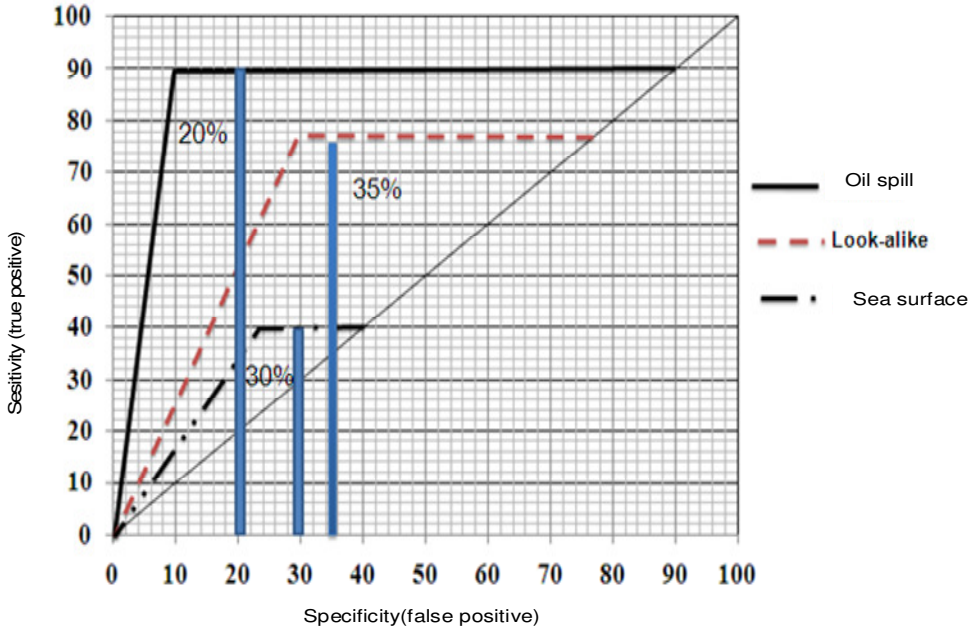

Figure 8. ROC for oil spill discrimination from look-alikes and sea surface roughness.

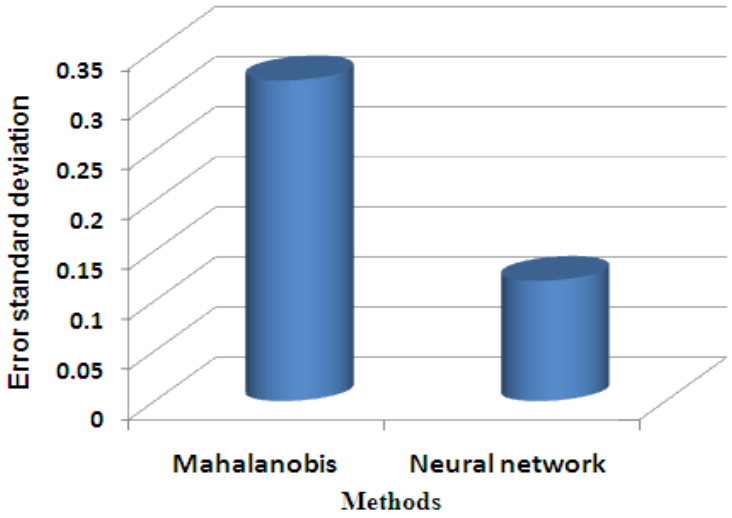

Figure 9. Standared error for different methods.

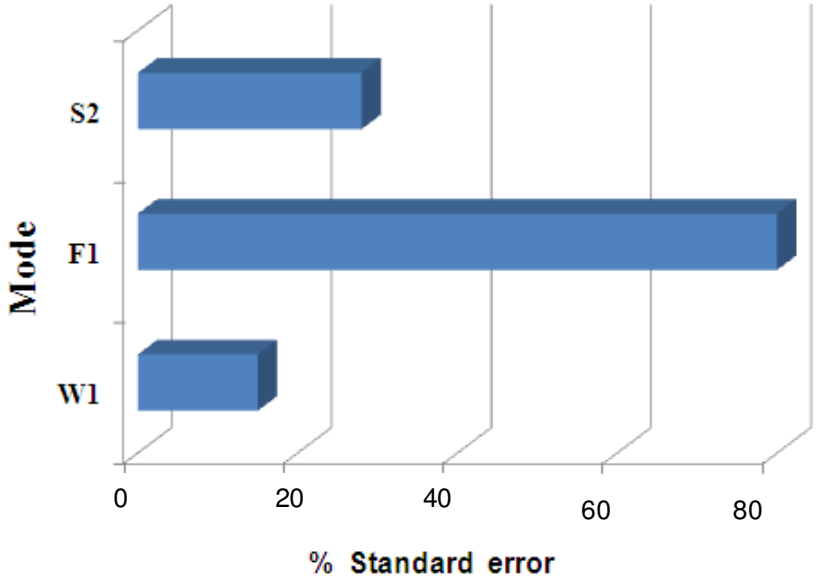

Figure 10. % Standared error for different modes.

number of its adaptive parameters (units and connections) has been carried out by using a pruning procedure. Accordingly, a network is examined to assess the relative importance of its weights, and the least important ones are deleted. Typically, this is followed by some further training of the pruned network, and the procedure of pruning and training may be repeated for several cycles. Clearly, there are various choices to be made concerning how much training is applied at each stage, what fraction of the weights is pruned, and so on. In the present work, every time a weight is removed, the new net is trained, as in the case of the initial training. The overall error value approaches a value of convergence, and, since the study started with a net committing no errors, the pruning procedure was continued until it was realized that new removals involve errors in the classification task. The most important consideration, however, is how to decide which weights should be removed. To do this, some measure of the relative importance was needed, or saliency of different weights. This result agrees with Topouzelis et al. (2009).

Figure 10 shows that W1 mode data has lower persentage value of standard error of 15% in comparison to F1 and S2 mode data. This means that W1 mode

perform better detection of oil spills than F1and S2 modes. In fact, the W1 mode showed steeper incident angle of 30° than the S1 and S2 modes. The offshore wind speed during the W1 mode overpass was 4.11 m/s, whereas the offshore wind speed was 7 m/s during the S2 mode overpass. Wind speeds below 6 m/s are appropriate for detection of oil spill in SAR data (Solberg and Volden, 1997). Therefore, applications requiring imaging of ocean surface, steep incidence angles are preferable as there is a greater contrast of backscatter manifested at the ocean surface (Marghany et al., 2009b; Marghany and Mazlan, 2010).

In contrast to previous studies of Fiscella et al. (2000) and Maged and Mazlan (2010), the Mahalanobis classifier provides classification pattern of oil spill where the slight oil spill can distinguish from meduim and heavy oil spill pixels. Neverthless, this study is consitented with Topouzelis et al. (2009). In consequence, the ANN extracted oil spill pixels automatically from surrounding pixels without using thresholding technique or different segemntation algorithm as stated at Solberg et al. (1999), Samad and Mansor (2002) and Marghany and Mazlan (2010).

CONCLUSION

This study has demostrated a compartive method for oil spill detection in RADARSAT-1 SAR different mode data. Two methods are involved:

(i) Post supervised classification (Mahalanobis Classification).
(ii) Neural network (NN).

The study shows that Mahalanobis classifier algorithm provides information about the level of oil spill occurrences in RADARSAT SAR data with accuracy of 87.8, and 92.7%. In terms of ROC area, it could be inferred that oil spill, look-alikes and sea surface roughness were perfectly discriminated, as provided by area difference of 20% for oil spill, 35% look–alikes and 30% for sea roughness. Finally, the results show that ANN distinguishes oil spill from surrounding sea surface features with standard deviation of 0.12. In conclusion, integration of different algorithms for oil spill detection provides better ways of getting the effective oil detection. The ANN algorithms is an appropriate algorithm for oil spill detection and while the W1 mode is appropriate for oil spill and look-alikes discrimination and detection using RADARSAT-1 SAR data.

REFERENCES

Aggoune ME, Atlas LE, Cohn DA, El-Sharkawi MA and Marks RJ (1989). Artificial neural networks for power system static security assessment. IEEE Int. Sym. Cir. Syst. Portland, Oregon, pp. 490-494.

Alpers W, Hühnerfuss H (1988). Radar signatures of oil films floating on the sea surface and the marangoni effect. J. Geophys. Res., 93: 3642-648.

Balick L, DiBenedetto JA, Lutz SS (1997). Fluorescence emission spectral measurements for the detection of oil on shore. Environmental research institute of Michigan, Ann Arbor, Michigan, I: 13-20.

Brekke C, Solberg A (2005). Oil spill detection by satellite remote sensing. Rem. Sens. Environ., 95: 1-13.

Dunnet G, Crisp D, Conan G, Bourne W (1982). Oil pollution and seabird populations. Philos. Trans. Royal Soc. London, B 297(1087): 413–427.

Fingas M (2001). The basics of oil spill cleanup. Lewis Publishers,New York.

Fingas MF, Brown CE (1997). Review of oil spill remote sensing. Spil. Sci. Tech. Bull., 4: 199–208.

Fiscella B, Giancaspro A, Nirchio F, Pavese P, Trivero P (2000). Oil spill detection using marine SAR images. Int. J. Rem. Sens., 21(18): 3561–3566.

Frate FD, Petrocchi A, Lichtenegger J, Calabresi G (2000). Neural networks for oil spill detection using ERS-SAR data. IEEE Trans. Geosci. Rem. Sens., 38(5): 2282–2287.

Hamzah A (1988). Malaysia's exclusive economic zone: A Study in Legal Aspects, Pelanduk Publications,Petaling Jaya,Selangor, Malaysia.

Hect-Nielsen R (1989). Theory of the back propagation neural network. Proc. Int. Joint Conf. Neu. Netw., June 1989, New York: IEEE Press, I : 593-611.

Hengsterman T, Reuter R (1990). Lidar fluorosensing of mineral oil spills on the sea surface. Appl. Opt., *29*: 3218-3227.

Holt B (2004). SAR imaging of the ocean surface. In Jackson CR and Apel JR (Eds.) synthetic aperture radar marine user's manual. Washington, DC7 NOAA NESDIS Office Res. Appl., pp. 25-81.

Marghany M (2001). RADARSAT automatic algorithms for detecting coastal oil spill pollution. Int. J. Appl. Ear. Obs. Geo., 3: 191–196.

Marghany M (2004). RADARSAT for oil spill trajectory model. Environ. Mod. Sof., 19: 473–483.

Marghany M (2010). Examining the least square method to retrieve sea surface salinity from MODIS satellite data. Eur. J. Sci. Res. 40 (30): 377-386.

Marghany M, Cracknell AP, Hashim M (2009a). Modification of fractal algorithm for oil Spill Detection from RADARSAT-1 SAR Data. Int. J. Appl. Ear. Obs. Geo., 11: 96-102.

Marghany M, Cracknell AP, Hashim M (2009b). Comparison between Radarsat-1 SAR different data modes for oil spill detection by a fractal box counting algorithm. Int. J. Dig. Ear., 2(3): 237-256.

Marghany M, Hashim M (2010). Texture entropy algorithm for automatic detection of oil spill from RADARSAT-1 SAR data. Int. J. Phy. Sci., 5(9): 1475-1480.

Marghany M, Hashim M, Cracknell AP (2007). fractal dimension algorithm for detecting oil spills using RADARSAT-1 SAR. In Gervasi O. and Gavrilova M. (Eds.): ICCSA, Springer-Verlag Berlin Heidelberg, Part I: 1054–1062.

Marghany M, Hashim M, Cracknell AP (2010). Modelling sea surface salinity from MODIS Satellite data. In Gervasi O and Gavrilova M (Eds.): ICCSA., 6016: 545-556.

Marghany M, Mazlan H (2005). Simulation of oil slick trajectory movements from the RADARSAT-1 SAR. Asian J. Geo., 5: 17–27.

Marghany M, Van Genderen J (2001). Texture algorithms for oil pollution detection and tidal current effects on oil spill spreading. Asian J. Geo., 1: 33–44.

Michael N (2005). Artificial intelligence: A guide to intelligent systems. 2nd editon, Harlow, England: Addison Wesley.

Migliaccio M, Gambardella A, Tranfaglia M (2007). SAR polarimetry to observe oil spills. IEEE Trans. Geosci. Rem. Sens., 45(2): 506-511.

Samad R, Mansor SB (2002). Detection of oil spill pollution using RADARSAT SAR imagery. CD Proceedings of 23rd Asian Conference on Remote Sensing, Birendra International Convention Centre in Kathmandu, Nepal, November 25 - 29, 2002, Asian Rem. Sens.

Shaw KE, Thomson GG (1973). The straits of Malacca in relation to problems of the Indian and Pacific Ocean, Univ. Edu. Press

Singapore, pp. 174-178.
Solberg AHS, Storvik G, Solberg R, Volden E (1999). Automatic detection of oil spills in ERS SAR images. IEEE Trans. Geosci. Rem. Sens., 37(4): 1916–1924.
Topouzelis K, Karathanassi V, Pavlakis P, Rokos D (2007). Detection and discrimination between oil spills and look-alike phenomena through neural networks. ISPRS J. Photo. Rem. Sens., 62: 264-270.
Topouzelis K, Karathanassi V, Pavlakis P, Rokos D (2009). Potentiality of feed-forward neural networks for classifying dark formations to oil spills and look-alikes. Geo. Int., 24(3): 179–219.
Topouzelis KN (2008). Oil spill detection by SAR images: Dark formation detection, feature extraction and classification algorithms. Sens., 8: 6642-6659.
Trivero P, Fiscella B, Gomez F, Pavese P (1998). SAR detection and characterization of sea surface slicks. Int. J. Rem. Sen., 19: 543–548.
Trivero P, Fiscella B, Pavese P(2001). Sea surface slicks measured by SAR, Nuo. Cim., 24C: 99-111.
Zeynalova M, Rustamov R, Salahova S (2009). Advanced space technology for oil spill detection. Springer Science, New York.